Solar Energy Materials and Solar Cells 188 (2018) 182–189

Contents lists available at ScienceDirect

Solar Energy Materials and Solar Cells

journal homepage: www.elsevier.com/locate/solmat

Explorative studies of novel silicon surface passivation materials: Considerations and lessons learned

L.E. Black[a,1], B.W.H. van de Loo[a,b,1], B. Macco[a,1], J. Melskens[a,*,1], W.J.H. Berghuis[a], W.M.M. Kessels[a]

[a] Department of Applied Physics, Eindhoven University of Technology, P.O. Box 513, 5600 MB Eindhoven, The Netherlands
[b] Tempress Systems BV, Vaassen 8171 MD, The Netherlands

ARTICLE INFO

Keywords:
Surface passivation
Silicon
Solar cells
Atomic layer deposition (ALD)
Passivating contacts

ABSTRACT

Despite the existence of several highly effective and well-characterized passivating materials for crystalline silicon surfaces, the topic of surface passivation and the investigation of new passivating materials remain of considerable interest for silicon photovoltaics research. However, the question of whether and under what circumstances a particular material will provide effective surface passivation remains difficult to answer. In this work, we provide an overview of recent insights relating to this question, drawing from our own work on novel passivation materials including MoO_x, Nb_2O_5, TiO_x, ZnO, and PO_x, and illustrated with experimental results. Factors that strongly influence the passivation performance include the use of pre-grown interfacial oxides, the film thickness, the annealing conditions, and the presence of capping layers. The impact of these factors on the surface passivation can vary widely from material to material. Therefore, all of these factors should be taken into account when investigating potential new surface passivation materials.

1. Introduction

Effective surface passivation is critical to realizing high-efficiency crystalline silicon (c-Si) solar cells and is becoming ever more important as wafer thicknesses are reduced and bulk Si quality improves. At the same time, new demands on the functionality of passivation layers have emerged, such as the ability to form passivating contact structures that in addition to passivation, enable the selective extraction of either positive or negative charges from the Si bulk [1,2]. These demands have stimulated significant research efforts aimed at evaluating the passivation properties of novel materials [1–9]. As a result, in the last decade, the list of materials known to be capable of effectively passivating c-Si surfaces has expanded significantly. The well-established Si-based passivation layers (SiO_2 [10], SiN_x [11], a-Si:H [12], and more recently proven Al_2O_3 [13–16]) have been joined by a range of new materials including HfO_2 [15,17,18], TiO_x [19–23], Ta_2O_5 [24] and Ga_2O_3 [25–27], and new passivation materials continue to be reported, such as ZnO [28], Nb_2O_5 [29, 84], PO_x [30,85], and ZrO_x [31]. Table 1 gives a summary of state-of-the-art passivation results for these materials and a few other notable examples. Note that some of these passivation materials can also serve as passivating contacts, as apart from preventing minority carrier recombination at the c-Si surface, they also yield a sufficiently low contact resistance to c-Si for majority carriers. In Fig. 1, transmission electron microscopy (TEM) images for a selection of these passivating materials are shown.

The mechanism of surface passivation is generally understood to involve a reduction in the number of interface states (“chemical” passivation) and/or suppression of the concentration of either electrons or holes at the semiconductor surface (historically referred to as “field-effect” passivation) (in general, effective passivation almost always involves a combination of these two mechanisms). However, the reasons for when and why a particular material will provide passivation are still not entirely clear. Some materials that were long believed not to provide effective surface passivation have now been shown to do so under the right conditions. For instance, TiO_x was replaced by SiN_x as the preferred anti-reflection coating (ARC) for c-Si solar cells in the late 1990s due to the more effective passivation provided by SiN_x, but it has recently been shown that TiO_x can in fact also provide excellent passivation [19–23]. On the other hand, other materials that are potentially relevant to c-Si photovoltaics thus far do not seem to provide passivation, regardless of their preparation method and post-deposition treatment. However, the growing number of studies of different

* Corresponding author.
E-mail addresses: l.e.black@tue.nl (L.E. Black), j.melskens@tue.nl (J. Melskens).
[1] Equally contributing authors.

https://doi.org/10.1016/j.solmat.2018.07.003
Received 19 February 2018; Received in revised form 5 June 2018; Accepted 2 July 2018
Available online 11 September 2018

Table 1
Selection of state-of-the-art passivation results reported for various passivation materials on *n*-type substrates with a bulk resistivity in the range of 1–7 Ω cm (unless otherwise specified). $S_{eff,max}$ values are calculated from the original lifetime data assuming an infinite bulk lifetime. In general we have selected the references with the lowest reported $S_{eff,max}$ in this resistivity range, giving preference to reports on more highly doped substrates in case of similar values. Representative values for the bandgap are given (additional references for these bandgap values have been included in cases where these are not mentioned in the reference for $S_{eff,max}$). The typical polarity (*n* or *p*) of the induced silicon space-charge region is specified. n^+ or p^+ indicate particularly strong band bending in the silicon, while *p/n* indicates that band bending is tunable through doping. We also specify the passivation layer thickness and whether a pre-grown SiO_x interlayer (either thermally or chemically grown) was present. Materials that are capable of forming passivating contacts for electron or holes are indicated.

Material	Bandgap (eV)	$S_{eff,max}$ (cm/s)	Induced surface charge	Preparation Method	Pre-grown SiO_x	Thickness (nm)	Remarks	Ref.
SiO_2	9[a]	2.4	*n*	Thermal oxidation	–	~110		[32]
SiN_x	1.8–5.3[a]	3.5	n^+	PECVD	–	> 50	Common ARC/passivation for n^+ Si in homojunction cells	[33]
a-Si:H	1.6–1.8	0.7	*p/n*	PECVD	–	280	*p*- or *n*-doping possible Can form e- or h-contact	[34]
poly-Si	~1.1[a]	0.4	*p/n*	LPCVD	therm.	150	*p*- or *n*-doping possible Can form e- or h- contact	[35]
Al_2O_3	6.4[a]	1.3	p^+	ALD	–	30	Common passivation for p^+ Si in PERC cells	[36]
PO_x	> 5	2.7	n^+	ALD	–	6		[30]
HfO_2	5.3–5.7	3.3	*n*	ALD	–	15		[18]
Ta_2O_5	4.4[a]	6.1	*p*	ALD	–	12		[24]
TiO_x	3.5	3.7	*p*	ALD	–	15	Former use as ARC. Can form e-contact	[21]
Ga_2O_3	4.2–5.2	6.4	p^+	ALD	–	4.5		[25]
MoO_x	2.8	29	p^+	ALD	chem.	10	Can form h-contact with a-Si:H	This work
Nb_2O_5	3.6	6.8	p^+	ALD	chem.	5	Can form e-contact	[29]
AlN	6.2	12[b]	*p*	Sputtering	chem.	50		[37]
ZnO	> 3	8.5	*n*	ALD	chem.	73	Common TCO, *n*-doping possible	[28]
ZrO_x	5–6	9.1	*p*	ALD	–	20		[31]

(ARC = Anti-reflection coating; TCO = Transparent conductive oxide).
[a] Values taken from Ref. [1] for SiO_2, poly-Si, and Ta_2O_5, Ref. [38] for SiN_x, and Ref. [16] for Al_2O_3.
[b] Obtained on 1 Ω cm *p*-type Si.

materials means that significantly more data relating to this question are becoming available.

In our group, we have investigated a large number of materials prepared by atomic layer deposition (ALD) for surface passivation of c-Si. ALD provides distinct advantages for surface passivation studies, such as large-area uniformity, precise thickness control, and damage-free ('soft') deposition [7]. Materials that have recently been examined include Nb_2O_5, PO_x, ZnO, TiO_x, and MoO_x. In this work, we will highlight several trends and exemplary cases taken from these and other datasets which provide insight into the factors that are important to surface passivation, with a particular emphasis on results that deviate from or go beyond conventional wisdom. While such examples do not yet permit us to outline a step-by-step procedure for reliably achieving surface passivation with new materials, they do highlight some important factors that ought to be taken into account when investigating novel materials for surface passivation properties. In particular we will highlight the role of pre-grown interfacial oxides (prepared by e.g. a standard Radio Corporation of America (RCA) clean or a low-temperature oxidation), the existence of different optima for film thickness, variation in optimum annealing temperature between different materials, and the potential role of capping layers in providing hydrogen for interface passivation. Since there are already a number of recent works which review passivating materials and/or passivating contacts [1–9], this work is not intended as a fully exhaustive review paper, but is instead primarily focused on providing the latest insights taken from a variety of relatively new passivation materials.

2. Experimental

As substrates for the ALD films discussed in this study we used double-side-polished (100) 1–5 Ωcm *n*-type floatzone (FZ) Si wafers. Films were deposited by ALD in Oxford Instruments FlexAL (in case of Nb_2O_5 [29], TiO_x [43], and Al_2O_3 [44]) or OpAL (in case of MoO_x [42,45] and H, Al or B doped ZnO [46-48]) reactors. Annealing was performed using a Jipelec rapid thermal annealing system. The passivation quality was assessed by transient and quasi-steady-state photoconductance (QSSPC) measurements using a Sinton WCT-120TS lifetime tester. Film thickness was evaluated using a J.A. Woollam M2000U variable angle spectroscopic ellipsometer.

3. Results

3.1. Surface preparation and the role of pre-grown interfacial oxides

The conventional silicon surface preparation procedure prior to surface passivation involves one or several wet-chemical cleaning steps (e.g. a Radio Corporation of America (RCA) standard clean [49]) which typically results in the growth of a thin (1–2 nm) surface oxide. Immediately before the deposition of a passivating film, this oxide is removed by etching in dilute hydrofluoric acid (HF) to leave a hydrophobic, hydrogen-terminated surface. The latter is generally considered the ideal starting surface for passivation, as such low-temperature wet chemical oxides are generally regarded as being of low-quality — usually they provide negligible passivation on their own — and their removal enables the formation of a new high-quality interface. This is well-established for example for thermal SiO_2 [50], PECVD SiN_x [51] and PECVD a-Si:H [34]. Note that, at least in the case of oxide materials, the formation of this new interface generally involves the growth of a new interfacial SiO_x layer either during deposition or upon subsequent annealing, (as visible in the TEM images shown in Fig. 1 of Al_2O_3, TiO_x, and Nb_2O_5 deposited on HF-treated Si), where the thickness and other properties of this layer will depend on the specific processing conditions and interfacial chemistry.

Contrary to this picture, we have found that in some cases retaining the oxide grown during surface cleaning, or intentionally growing a thin chemical oxide, can be beneficial for surface passivation by metal

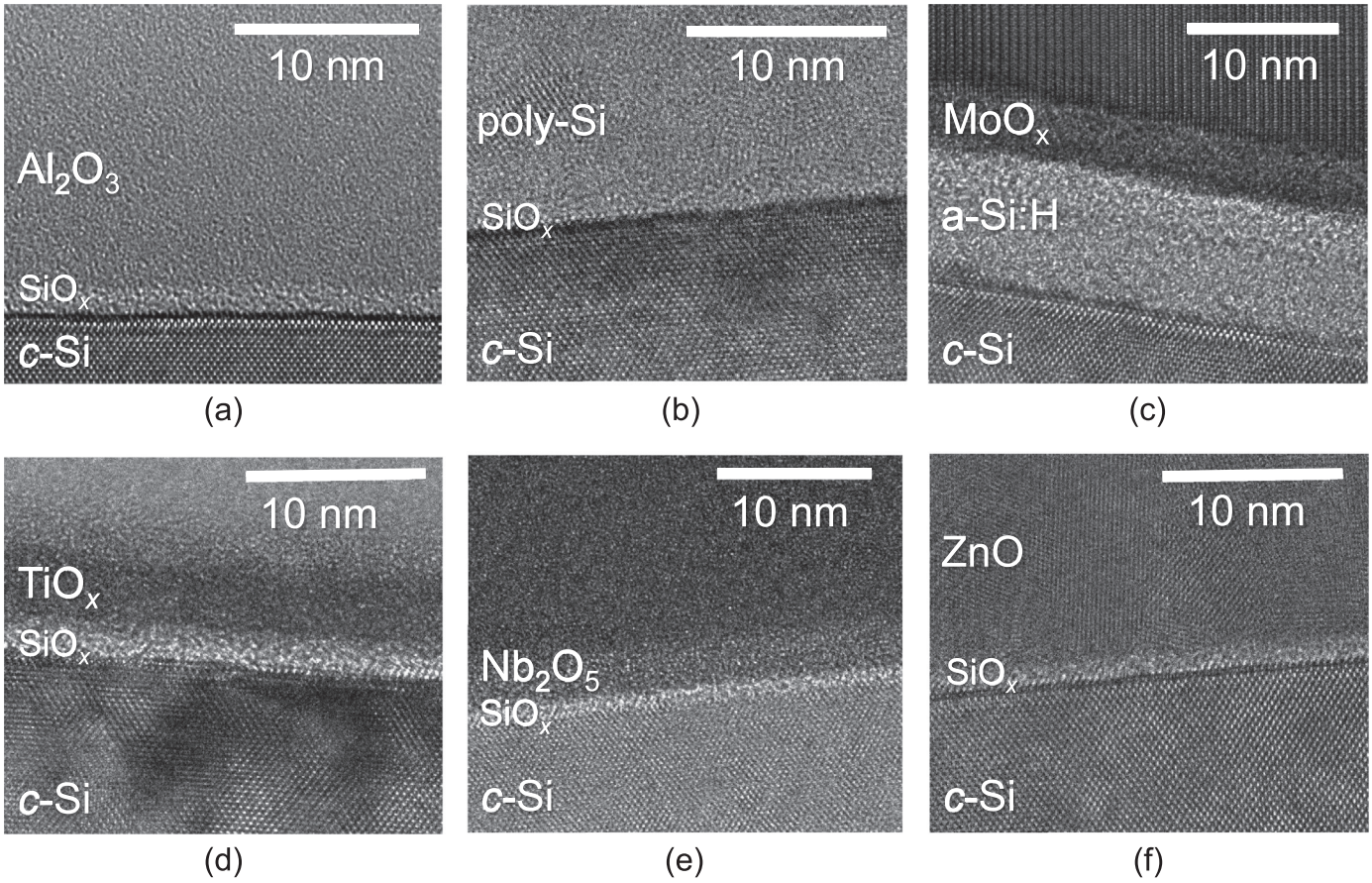

Fig. 1. Cross-sectional bright-field transmission electron microscopy images of various surface passivation materials on *n*-type c-Si (100). (a) ALD Al_2O_3 prepared at 200 °C on HF-treated Si after a 450 °C forming gas anneal (FGA) [13]. (b) *p*-type poly-Si on SiO_x prepared by low-temperature oxidation [39]. (c) ALD MoO_x on a-Si:H prepared by chemical vapor deposition [40] and capped with ALD In_2O_3:H [41], after annealing at 200 °C in N_2 [42]. (d) ALD TiO_x prepared at 200 °C on HF-treated Si (e) ALD Nb_2O_5 prepared at 150 °C on HF-treated Si and subjected to a 300 °C FGA [29] (f) ALD boron-doped ZnO prepared at 200 °C on c-Si with an RCA oxide and subjected to a 450 °C FGA.

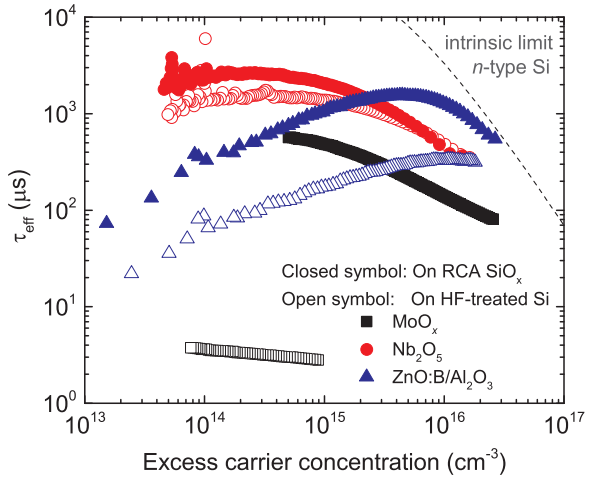

Fig. 2. Effective excess carrier lifetime for 10 nm ALD MoO_x films, 5 nm ALD Nb_2O_5 films, or 75/30 nm boron-doped ZnO/Al_2O_3 stacks prepared at 200 °C on *n*-type Si (3.3 Ω cm), either HF-treated or with an RCA oxide. The Nb_2O_5 sample was prepared at 150 °C, whereas the MoO_x and the boron-doped ZnO/Al_2O_3 samples were prepared at 200 °C. The MoO_x and Nb_2O_5 films were subjected to 1 h optimized post-deposition FGA treatments of 1 and 2 h at 300 °C, respectively. The ZnO:B/Al_2O_3 stacks received a 30 min FGA at 450 °C.

oxides. In fact, using a starting surface with an existing thin oxide layer can sometimes even result in passivation in cases where the same procedure applied to a HF-treated surface would not. For instance, MoO_x, which is being explored as hole-selective contact [52, 56, 57], is a material which typically yields very poor surface passivation when directly applied to the Si surface [54-57]. For this reason, it is either used as partial rear contact [56] or combined with a dedicated amorphous silicon passivation layer [52,53] as shown in Fig. 1(c). However, we recently found that MoO_x prepared by ALD [42,45] can yield surface passivation when it is deposited on an RCA oxide and subsequently subjected to a forming gas anneal (FGA) treatment. This is shown in Fig. 2. These results suggest that the interfacial oxide between MoO_x and HF-treated silicon — that naturally forms during processing — is of poor quality and that this interfacial oxide cannot be made to passivate by an FGA treatment. Conversely, the well-defined RCA oxide can be used to achieve passivation by MoO_x, with the best results being obtained after a one hour FGA treatment at 300 °C.

The beneficial effects of an RCA oxide are also observed for ALD ZnO:B/Al_2O_3 stacks. Such stacks yield only moderate levels of passivation on HF-treated Si surfaces, whereas excellent passivation is achieved on an RCA oxide (see Fig. 1(f)). Therefore, also in the case of ALD ZnO it seems that the oxide that forms during deposition on HF-treated Si is not of high quality. Conversely, for ALD Nb_2O_5 good passivation is achieved on both HF-treated Si and Si with an RCA SiO_x layer. This shows that for this process a SiO_x layer is formed during deposition and post-deposition annealing that enables good surface passivation [29]. This interfacial SiO_x layer is also visible in Fig. 1(e).

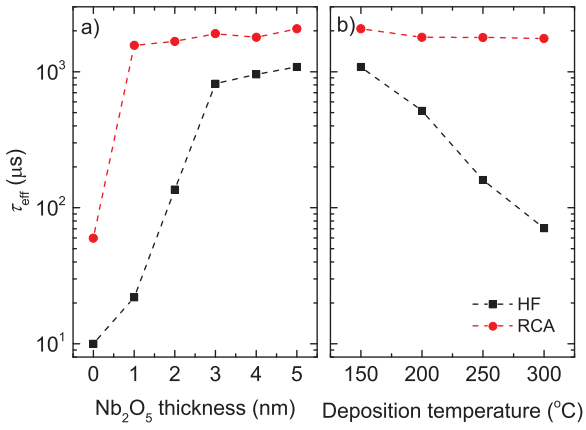

Fig. 3. Effective excess carrier lifetime at an excess carrier concentration of 10^{15} cm^{-3} for *n*-type Si (3 Ωcm) after 2 h of FGA at 300 °C (a) as a function of Nb_2O_5 film thickness using a deposition temperature of 150 °C and (b) as a function of deposition temperature for 5 nm thick films.

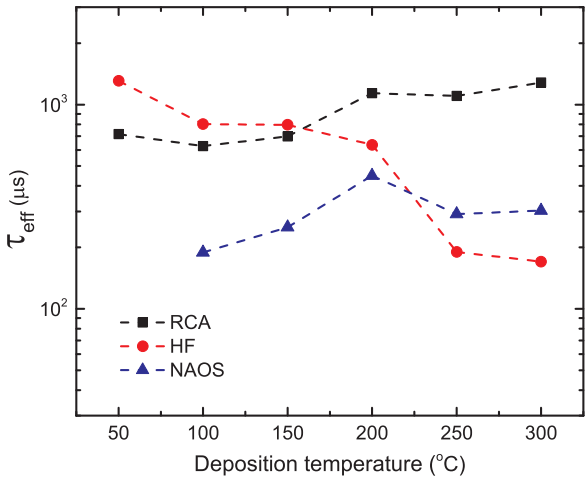

Fig. 4. Effective excess carrier lifetime at an excess carrier concentration of 10^{15} cm^{-3} versus deposition temperature for *n*-type Si (3 Ω cm), either HF-treated, or with an RCA or NAOS oxide, and passivated by 5 nm of TiO_x. Samples were annealed at 300 °C in forming gas. The lifetime reported for each sample is the value obtained following stepwise annealing. The annealing times (13–180 min) are optimized for each sample.

The use of a chemical oxide can also strongly alter the passivation behavior of materials that do provide passivation to HF-treated Si. This is clearly illustrated by the case of ALD Nb_2O_5 [29]. On HF-treated Si, the surface passivation quality improves when using thicker Nb_2O_5 films and lower deposition temperatures, as shown in Fig. 3. However, the use of an RCA oxide not only yields a better passivation quality, but in addition it renders the passivation level much less dependent on the experimental conditions. Strikingly, this even enables excellent passivation of the surface using only 1 nm of ALD Nb_2O_5. The sensitivity of the passivation quality on HF-treated Si surfaces to the experimental conditions is thought to originate from differences in the formation of the interfacial oxide during deposition [29]. It is known that SiO_x interfaces formed by different chemical processes [58] and by the same process at different temperatures (e.g. thermal oxidation [59]) can exhibit significant differences in interface state and fixed charge densities, which determine passivation quality. Conversely, the fact that the interfacial oxide is formed prior to Nb_2O_5 deposition in the case of RCA-treated surfaces renders such surfaces much less sensitive to the exact process conditions.

The nature of the pre-grown oxide is also important. Ultrathin oxides may be prepared by a wide variety of methods, including growth in air (native), wet-chemical (e.g. nitric acid oxidation (NAOS), RCA, boiling water), UV/ozone, O_2 plasma, and thermal oxidation, and these can yield significantly different levels of surface passivation [60–67]. An example of this can be seen from the comparison of lifetimes for TiO_x-passivated samples with RCA and NAOS oxides in Fig. 4, where the RCA oxide results in significantly better passivation than the NAOS. Note that, based on our own data and that of others, it does not so far appear possible to establish a simple generally applicable correlation between the readily observable macroscopic properties (thickness, stoichiometry/oxidation state) of a given SiO_x layer (whether pre-grown or formed during processing) and its suitability for passivation, so that this needs to be tested directly in each case.

Note that beneficial effects from pre-grown interfacial oxides have been reported before. For example, Mihailetchi *et al.* reported that the use of a 1.5 nm oxide grown by NAOS enabled effective passivation of p^+ Si surfaces by PECVD SiN_x [68]. Ultrathin oxides are also routinely employed as interlayers in polycrystalline silicon (poly-Si) passivating contacts [69–72].

While the use of a pre-grown oxide can enable passivation in some cases, in other cases an HF-treated starting surface results in better passivation, as seen for example for the TiO_x films deposited at 50 °C in Fig. 4. This is also generally the case for ALD Al_2O_3 which provides a better surface passivation quality on HF-treated silicon in comparison to chemically pre-oxidized silicon [73]. Generally, it appears that some materials and some deposition processes are capable of forming their own high-quality interfaces, while others benefit from the presence of a pre-formed oxide interface. Therefore, the influence of the starting surface needs to be investigated for different materials and processes on an individual basis.

3.2. Influence of film thickness

The thickness of a passivation layer is another known parameter affecting passivation quality. It is conventionally expected that very thin films will provide worse passivation than thicker films. More specifically, the passivation quality is usually observed to improve with film thickness up to a certain point (typically ~10 nm) and then to saturate. This is well-established for example for thermal SiO_2 [50], PECVD SiN_x [51], and ALD Al_2O_3 [74–76]. At least in case of Al_2O_3, which owes its excellent passivation partly to a strong field-effect passivation, it is the chemical passivation which deteriorates when moving to very thin films [77]; this may also apply to other passivating materials. Note that for a-Si:H, saturation in fact appears not to occur even for thicknesses up to several hundred nm, but the passivation quality is still observed to improve monotonically with thickness [34].

In contrast to this simple picture, we have found that for some materials passivation is not a monotonic function of film thickness. In certain cases there is a clear optimum at a relatively low thickness value, as is illustrated in Fig. 5 for TiO_x after an FGA treatment. A similar optimum thickness behavior was also observed for TiO_x by Yang *et al.* who also used an FGA treatment [22,23]. Consequently, if only relatively thick films had been investigated in these cases, as is often the case, passivation would have appeared considerably worse.

Our results and those of Yang *et al.* [22,23] are in contrast to those of Cui *et al.*, who used an N_2 annealing treatment and observed saturation of passivation for TiO_x thicknesses between ~8 and 63 nm, which resembles the classical case where the passivation quality saturates above a certain layer thickness [21]. Therefore, the thickness dependence of passivation appears not to be an intrinsic property of TiO_x, but depends on the processing history of the films. Since each of these studies employed different ALD precursors, deposition temperatures, and annealing treatments, these may account for the difference in passivation behavior.

Alternatively, for some materials saturation may occur, but much more rapidly than for SiO_2 or Al_2O_3. Indeed saturation of passivation

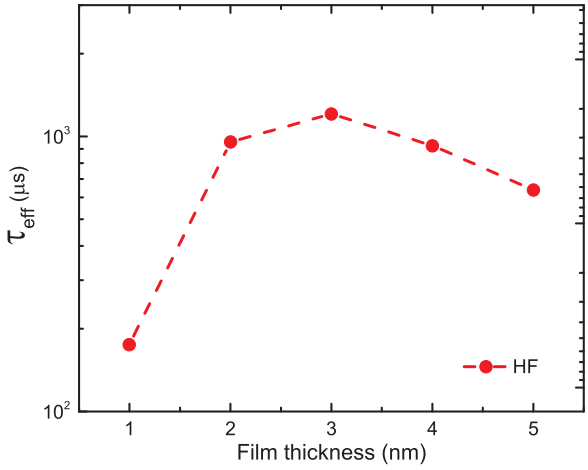

Fig. 5. Effective excess carrier lifetime at an excess carrier concentration of 10^{15} cm^{-3} versus TiO_x film thickness on HF-treated *n*-type Si (3 Ω cm). The TiO_x films were deposited at 200 °C. Annealing was performed at 300 °C in forming gas in a stepwise fashion. The optimum value attained in this way is reported for each thickness.

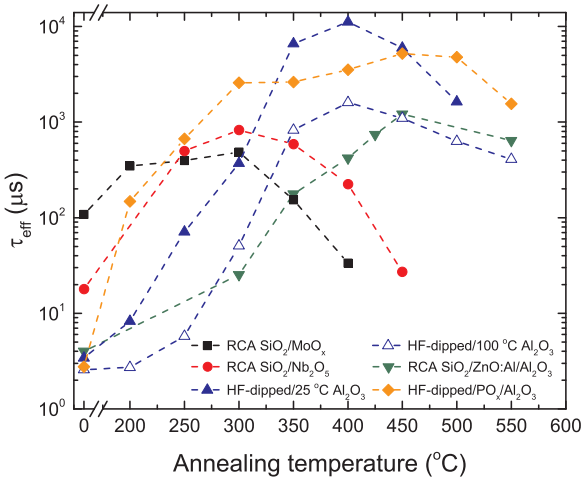

Fig. 6. Effective excess carrier lifetime at an excess carrier concentration of 10^{15} cm^{-3} versus annealing temperature for various passivating layers or layer stacks on *n*-type Si (either HF-treated or with an RCA oxide). Annealing was performed in forming gas (N_2/H_2) or N_2 in a stepwise fashion. For ZnO, the annealing was done in steps of 5 min in forming gas, while 1 h annealing steps were used in case of MoO_x and Nb_2O_5; the Al_2O_3 and PO_x/Al_2O_3 samples were annealed in N_2 in steps of 10 min. The MoO_x, Nb_2O_5 and Al_2O_3 films were 10, 5, and 14 nm thick, respectively. The ZnO:Al/Al_2O_3 and PO_x/Al_2O_3 stacks had film thicknesses of 75/30 and 6/14 nm, respectively.

can occur after only a few monolayers for some materials. An example of this was shown in Fig. 3, where passivation by Nb_2O_5 apparently saturates already after 1 nm on RCA oxide surfaces. Film thickness can therefore influence passivation in unexpected ways and the influence of film thickness on passivation should be carefully considered especially when investigating new materials.

3.3. Post-deposition annealing: Temperature optima and the role of capping layers

It is well-known that a post-deposition annealing treatment, either in N_2 or in a hydrogen-containing gas mixture (FGA), can improve the surface passivation quality. This is for instance the case for materials such as SiO_2, a-Si:H, SiN_x, and Al_2O_3 [16]. The general aim of such an annealing treatment is to effectively hydrogenate and passivate the dangling bonds present at the silicon surface, i.e. to improve the chemical passivation. Generally, a sufficiently high temperature has to be applied to enable the diffusion of hydrogen from either the passivating film itself or from a hydrogen-containing ambient (e.g. forming gas) towards the silicon interface, while at the same time avoiding excessive hydrogen loss from the film via effusion. In the case of both SiO_2 and Al_2O_3, the optimal annealing temperature is known to be close to 400 °C [16], while much lower temperatures around 180 °C appear optimal for a-Si:H [78]. This already indicates that the optimal annealing temperature may vary from material to material.

This point is made even more obvious when looking at the wide range of novel passivating materials, as is shown in Fig. 6. It is striking to see that the optimal annealing temperatures for MoO_x, Nb_2O_5, Al_2O_3, ZnO:Al, and PO_x are all different, indicating different annealing kinetics for each of these materials. It should be noted that since the annealing step time was not equal for all of the materials, a one-to-one comparison cannot be made for all the materials in this graph. Nonetheless, the observed trends should still be dominated by the temperature rather than by the anneal step time, since the rate of thermally-activated processes depends much more strongly on temperature. This is for example seen in the case of SiO_2/Al_2O_3 stacks, where the apparent saturated level of passivation differs for different annealing temperatures [79].

When comparing the three samples on the RCA oxide, i.e. MoO_x, Nb_2O_5, and ZnO:Al/Al_2O_3, it can be seen that the ZnO:Al/Al_2O_3 sample has a much higher onset and optimum temperature. This is striking if one assumes that the annealing kinetics depend on the hydrogenation reaction at the interface, as it is the same RCA SiO_x interface that needs to be passivated during the anneal treatment. These differences are therefore likely linked to differences in the kinetics of hydrogen diffusion through the material and toward the interface and effusion of hydrogen from the material. Conceivably, the transport of hydrogen takes place more readily and at lower temperatures in the amorphous MoO_x and Nb_2O_5 films as compared to the polycrystalline ZnO/Al_2O_3 stack. Since diffusion plays a role, film thickness is also likely to play a role in the exact annealing trend. Also material stability and possible crystallization during annealing can play an important role in degradation at higher temperatures and thus the location of the optimum. For the case of MoO_x, macroscopically visible formation of etch pits as well as a reduction of the material from near-stoichiometric MoO_3 to MoO_2 was observed by XPS when performing FGA treatments exceeding 300 °C, explaining the strong reduction in lifetime observed.

Capping of passivation layers prior to annealing by other materials, most notably Al_2O_3 and SiN_x, has proven to be a highly successful approach to improve or enable passivation. As illustrated in Fig. 7, it has for example been demonstrated that applying an Al_2O_3 capping layer can greatly enhance the passivation provided by ALD SiO_2, SiO_x/poly-Si, and SiO_x/ALD ZnO. For SiO_2 and poly-Si, it has been shown that the Al_2O_3 layer serves both as a hydrogen source and a hydrogen effusion barrier [78,80,81]. Note that hydrogen effusion barriers can also be formed by other materials, such as SiN_x [82]. Conversely, in the case of ALD ZnO, ample hydrogen for passivation is already present at the SiO_x interface and in the ZnO layer after the ALD process. In this case, the Al_2O_3 capping layer merely serves as a hydrogen effusion barrier that prevents a significant effusion of hydrogen at 400 °C [28].

However, the success of such Al_2O_3 capping layers does not necessarily translate to other passivation materials, as Fig. 7 shows for the cases of Nb_2O_5, MoO_x and TiO_x. For these three materials, the addition of the Al_2O_3 capping layer leads to a strong reduction in passivation. In the case of MoO_x capped with Al_2O_3, the deterioration is likely related to the visible formation of blisters when annealing at 300 °C. Such blistering was not observed for Nb_2O_5 and TiO_x capped by Al_2O_3, and the precise reasons for the detrimental effect of capping by Al_2O_3 are so far not known. Conceivably, the photocatalytic nature of both TiO_x and Nb_2O_5 plays a role. Both TiO_x and Nb_2O_5 yield improved passivation upon light soaking, which is thought to originate from an enhanced

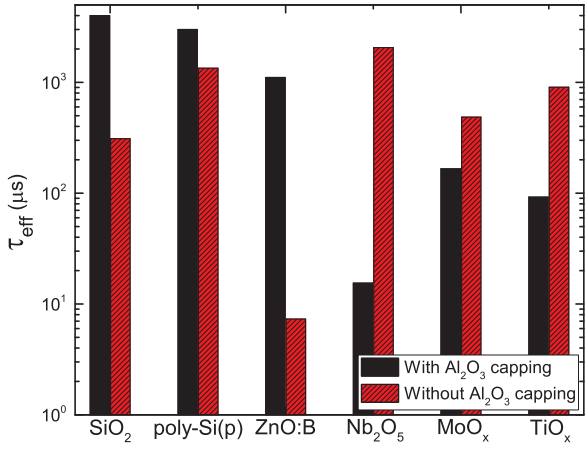

Fig. 7. Effective excess carrier lifetime at an excess carrier concentration of 10^{15} cm^{-3} for a variety of materials with and without capping by 30 nm thermal ALD Al_2O_3 after optimized annealing treatments (10 min at 400 °C in N_2 for SiO_2, 1 h at 400 °C in forming gas for poly-Si, 30 min at 450 °C in forming gas for ZnO:B, and 2 h, 1 h, and 30 min at 300 °C in forming gas for Nb_2O_5, MoO_x, and TiO_x, respectively). Data on ALD SiO_2 have been taken from [15]. poly-Si, ZnO [28], Nb_2O_5 and MoO_x were prepared on RCA SiO_x layers, while TiO_x layers were prepared on HF-treated Si.

field-effect passivation arising from more net negative fixed charge in the dielectric [20,29,83]. In the case of TiO_x, it has been argued that this enhancement of the negative charge upon light soaking originates from a photocatalytic reaction between the TiO_x surface and molecules from the ambient [83]. When an Al_2O_3 capping layer is applied, the photocatalytic surface of TiO_x or Nb_2O_5 is no longer exposed to the ambient. Therefore, such light-induced charging would be hindered, resulting in a lower field-effect passivation.

4. Discussion

We have shown how the choice of starting surface, the film thickness, and the use of capping layers can all be critical for achieving surface passivation by deposited layers. While we have considered these factors separately, we should stress that in reality different factors can be intertwined. The use of a pre-grown tunnel oxide can be very beneficial for TiO_x passivation at one deposition temperature for example, but for another deposition temperature it can give poor results. The point is that all of these factors need to be considered when investigating new materials for surface passivating properties.

The corollary to this point is that it is much harder to say with confidence that a material does not passivate — the negative case — than to confirm the positive case that it does. It may simply be that one has not yet found the necessary combination of surface pretreatments, process settings, and post-deposition treatments to achieve passivation. There is more than one example of a material known now to be effective for passivation that was written off in initial investigations.

Of course additional factors not discussed in this work, but well-known to affect passivation, including the substrate dopant density and orientation, the details of the deposition process (temperature, pressure, chemistry, etc.) and the presence of extrinsic doping in the passivating film, will also be highly important. In this work we have confined ourselves to aspects that appeared to us to be not so widely appreciated or documented in the literature, and which we could illustrate with our own data.

It should also be noted that, while we have talked broadly in terms of achieving or not achieving passivation, optimized passivation quality varies significantly between different materials and processes, as can be seen from an examination of the lifetime values reported throughout this work. Passivation quality is of course also not the only criterion that needs to be considered for device applications; optical properties, process compatibility, and environmental stability, among other factors, are all important. A low contact resistivity is an additional criterion important for materials intended for passivating contact applications [1]. However, the relevance of these latter aspects depends in the first place on effective surface passivation, underlining this as a key design criterion for all layers in direct contact with the silicon surface in c-Si solar cells.

5. Conclusions

Silicon surface passivation remains a highly important research topic, which has lately also been illustrated by the surging interest in passivating contact materials. This emerging field has prompted the investigation of numerous novel materials for silicon surface passivation. For many of these materials, it seems that considerations relevant to passivation such as starting surface, film thickness, annealing treatment, and the role of capping layers come into play in ways that sometimes run counter to conventional assumptions. In this work, we have explored these considerations both for more conventional and for recently-discovered passivation materials including MoO_x, ZnO, TiO_x, PO_x, and Nb_2O_5.

The main conclusion that can be drawn from this exploration is the fact that all these considerations strongly influence the passivation performance of most passivation materials. In addition, the optimal choice of one experimental parameter is also often found to depend on the choice of another. Therefore, the interdependence of all these factors needs to be carefully considered when investigating new materials for surface passivating properties. These lessons can prove useful in the design and optimization of future passivation schemes and passivating contacts for c-Si solar cells.

Acknowledgements

The authors gratefully acknowledge the Top consortia for Knowledge and Innovation Solar Energy programs "AAA" (grant 1409104), "RADAR" (grant TEUE116905), and "COMPASS" (grant TEID215022) of the Ministry of Economic Affairs of the Netherlands for financial support. The work of J. Melskens was supported by the Netherlands Organisation for Scientific Research under the Dutch TTW-VENI grant 15896. Marcel A. Verheijen is acknowledged for performing the TEM studies. Solliance and the Dutch province of Noord-Brabant are acknowledged for funding the TEM facility. Additionally, we would like to acknowledge J.H. Deijkers, V.H.M. Evers, and J. Palmans from Eindhoven University of Technology (Netherlands) for useful discussions and support during the experiments.

References

[1] J. Melskens, B.W.H. van de Loo, B. Macco, L.E. Black, S. Smit, W.M.M. Kessels, Passivating contacts for crystalline silicon solar cells: from concepts and materials to prospects, IEEE J. Photovolt. 8 (2) (2018) 373–388.
[2] J. Melskens, B.W.H. van de Loo, B. Macco, M.F.J. Vos, J. Palmans, S. Smit, W.M.M. Kessels, Concepts and prospects of passivating contacts for crystalline silicon solar cells, in: Proceedings of the 42nd IEEE Photovoltaic Specialists Conference, New Orleans, LA, USA, 2015, pp. 1–6.
[3] A. Cuevas, T.G. Allen, J. Bullock, Y. Wan, D. Yan, X. Zhang, Skin care for healthy silicon solar cells, in: Proceedings of the 42nd IEEE Photovoltaic Specialists Conference, New Orleans, LA, USA, 2015, pp. 1–6.
[4] C. Battaglia, A. Cuevas, S. de Wolf, High-efficiency crystalline silicon solar cells: status and perspectives, Energy Environ. Sci. 9 (2016) 1552–1576.
[5] J. Bullock *et al.*, Survey of dopant-free carrier-selective contacts for silicon solar cells, in: Proceedings of the 43rd IEEE Photovoltaic Specialists Conference, Portland, OR, USA, 2016, pp. 210–214.
[6] M. Hermle, Photovoltaic Solar Energy: From Fundamentals to Applications, in: A. Reinders, P. Verlinden, A. Freundlich (Eds.), 2017, pp. 125–135.
[7] B. Macco, B.W.H. van de Loo, W.M.M. Kessels, Atomic layer deposition for high-efficiency crystalline silicon solar cells, in: J. Bachmann (Ed.), Atomic Layer Deposition in Energy Conversion Applications, Wiley, 2017, pp. 41–99.
[8] P. Gao, Z. Yang, J. He, J. Yu, P. Liu, J. Zhu, Z. Ge, J. Ye, Dopant-free and carrier-selective heterocontacts for silicon solar cells: recent advances and perspectives,

Adv. Sci. (2017) 1–20 (no. 1700547).
[9] R.S. Bonilla, B. Hoex, P. Hamer, P.R. Wilshaw, Dielectric surface passivation for silicon solar cells: a review, Phys. Status Solidi A 214 (1700293) (2017).
[10] J.H. Zhao, A.H. Wang, M.A. Green, 24.5% efficiency silicon PERT cells on MCZ substrates and 24.7% PERL cells on FZ substrates, Prog. Photovolt.: Res. Appl. 7 (1999) 471–474.
[11] C. Leguijt, J.A. Eikelboom, A.W. Weeber, F.M. Schuurmans, W.C. Sinke, P.F.A. Alkemade, P.M. Sarro, C.H.M. Mar, L.A. Verhoef, Low temperature surface passivation for silicon solar cells, Sol. Energy Mater. Sol. Cells 40 (1996) 297–345.
[12] M. Schaper, J. Schmidt, H. Plagwitz, R. Brendel, 20.1%-efficient crystalline silicon solar cell with amorphous silicon rear-surface passivation, Prog. Photovolt.: Res. Appl. 13 (2005) 381–386.
[13] B. Hoex, S.B.S. Heil, E. Langereis, M.C.M. van de Sanden, W.M.M. Kessels, Ultralow surface recombination of c-Si substrates passivated by plasma-assisted atomic layer deposited Al_2O_3, Appl. Phys. Lett. 89 (042112) (2006).
[14] G. Agostinelli, et al., Very low surface recombination velocities on p-type silicon wafers passivated with a dielectric with fixed negative charge, Sol. Energy Mater. Sol. Cells 90 (18–19) (2006) 3438–3443.
[15] G. Dingemans, W.M.M. Kessels, Aluminum oxide and other ALD materials for Si surface passivation, ECS Trans. 41 (2) (2011) 293–301.
[16] G. Dingemans, W.M.M. Kessels, Status and prospects of Al_2O_3-based surface passivation schemes for silicon solar cells, J. Vac. Sci. Technol. A 30 (040802) (2012).
[17] F. Lin, B. Hoex, Y.H. Koh, J.J. Lin, A.G. Aberle, Low-temperature surface passivation of moderately doped crystalline silicon by atomic-layer-deposited hafnium oxide films, Energy Procedia 15 (2012) 84–90.
[18] J. Cui, Y. Wan, Y. Cui, Y. Chen, A. Cuevas, Highly effective electronic passivation of silicon surfaces by atomic layer deposited hafnium oxide, Appl. Phys. Lett. 110 (021602) (2017).
[19] A.F. Thomson, K.R. McIntosh, Light-enhanced surface passivation of TiO_2-coated silicon, Prog. Photovolt.: Res. Appl. 20 (2012) 343–349.
[20] B. Liao, B. Hoex, A.G. Aberle, D. Chi, C.S. Bhatia, Excellent c-Si surface passivation by low-temperature atomic layer deposited titanium oxide, Appl. Phys. Lett. 104 (253903) (2014).
[21] J. Cui, et al., Titanium oxide: a re-emerging optical and passivating material for silicon solar cells, Sol. Energy Mater. Sol. Cells 158 (2016) 115–121.
[22] X. Yang, P. Zheng, Q. Bi, K. Weber, Silicon heterojunction solar cells with electron selective TiO_x contact, Sol. Energy Mater. Sol. Cells 150 (2016) 32–38.
[23] X. Yang, Q. Bi, H. Ali, K. Davis, W.V. Schoenfeld, K. Weber, High-performance TiO_2-based electron-selective contacts for crystalline silicon solar cells, Adv. Mater. (2016) 1–7, https://doi.org/10.1002/adma.201600926.
[24] Y. Wan, J. Bullock, A. Cuevas, Passivation of c-Si surfaces by ALD tantalum oxide capped with PECVD silicon nitride, Sol. Energy Mater. Sol. Cells 142 (2015) 42–46.
[25] T.G. Allen, A. Cuevas, Electronic passivation of silicon surfaces by thin films of atomic layer deposited gallium oxide, Appl. Phys. Lett. 105 (031601) (2014).
[26] T.G. Allen, A. Cuevas, Plasma enhanced atomic layer deposition of gallium oxide on crystalline silicon: demonstration of surface passivation and negative interfacial charge, Phys. Stat. Sol. RRL 9 (2015) 220–224.
[27] T.G. Allen, Y. Wan, A. Cuevas, Silicon surface passivation by gallium oxide capped with silicon nitride, IEEE J. Photovolt. 6 (4) (2016) 900–905.
[28] B.W.H. van de Loo, Atomic-Layer-Deposited Surface Passivation Schemes for Silicon Solar Cells (Ph.D. thesis), Eindhoven University of Technology, 2017.
[29] B. Macco, L.E. Black, J. Melskens, B.W.H. van de Loo, W.J.H. Berghuis, M.A. Verheijen, W.M.M. Kessels, Atomic-layer deposited Nb_2O_5 as transparent passivating electron contact for c-Si solar cells, Sol. Energy Mater. Sol. Cells 184 (2018) 98–104.
[30] L.E. Black, W.M.M. Kessels, PO_x/Al_2O_3 stacks: highly effective surface passivation of crystalline silicon with a large positive fixed charge, Appl. Phys. Lett. 112 (201603) (2018).
[31] Y. Wan, J. Bullock, M. Hettick, Z. Xu, D. Yan, J. Peng, A. Javey, A. Cuevas, Zirconium oxide surface passivation of crystalline silicon, Appl. Phys. Lett. 112 (201604) (2018).
[32] M.J. Kerr, A. Cuevas, Very low bulk and surface recombination in oxidized silicon wafers, Semicond. Sci. Technol. 17 (2002) 35–38.
[33] F.W. Chen, T.-.T.A. Li, J.E. Cotter, PECVD silicon nitride surface passivation for high-efficiency n-type silicon solar cells, in: Proceedings of the 4th IEEE World Conference on Photovoltaic Energy Conversion, Waikoloa, HI, USA, 2006, pp. 1020–1023.
[34] D. Deligiannis, V. Marioleas, R. Vasudevan, C.C.G. Visser, R.A.C.M.M. van Swaaij, M. Zeman, Understanding the thickness-dependent effective lifetime of crystalline silicon passivated with a thin layer of intrinsic hydrogenated amorphous silicon using a nanometer-accurate wet-etching method, J. Appl. Phys. 119 (235307) (2016).
[35] U. Römer, R. Peibst, T. Ohrdes, B. Lim, J. Krügener, T. Wietler, R. Brendel, Ion implantation for poly-Si passivated back-junction back-contacted solar cells, IEEE J. Photovolt. 5 (2) (2015) 507–514.
[36] A. Richter, S.W. Glunz, F. Werner, J. Schmidt, A. Cuevas, Improved quantitative description of Auger recombination in crystalline silicon, Phys. Rev. B 86 (165202) (2012).
[37] G. Krugel, A. Sharma, W. Wolke, J. Rentsch, R. Preu, Study of hydrogenated AlN as an anti-reflective coating and for the effective surface passivation of silicon, Phys. Status Solidi RRL 7 (7) (2013) 457–460.
[38] J. Hong, W.M.M. Kessels, W.J. Soppe, A.W. Weeber, W.M. Arnoldbik, M.C.M. van de Sanden, Influence of the high-temperature "firing" step on high-rate plasma deposited silicon nitride films used as bulk passivating antireflection coatings on silicon solar cells, J. Vac. Sci. Technol. B 21 (5) (2003) 2123–2132.
[39] M. Schnabel, B.W.H. van de Loo, W. Nemeth, B. Macco, P. Stradins, W.M.M. Kessels, D.L. Young, Hydrogen passivation of poly-Si/SiO_x contacts for Si solar cells using Al_2O_3 studied with deuterium, Appl. Phys. Lett. 112 (203901) (2018).
[40] B. Macco, J. Melskens, N.J. Podraza, K. Arts, C. Pugh, O. Thomas, W.M.M. Kessels, Correlating the silicon surface passivation to the nanostructure of low-temperature a-Si: H after rapid thermal annealing, J. Appl. Phys. 122 (35302) (2017).
[41] B. Macco, H.C.M. Knoops, W.M.M. Kessels, Electron scattering and doping mechanisms in solid phase crystallized In_2O_3: H prepared by atomic layer deposition, ACS Appl. Mater. Interfaces 7 (30) (2015) 16723–16729.
[42] B. Macco, M.F.J. Vos, N.F.W. Thissen, A.A. Bol, W.M.M. Kessels, Low-temperature atomic layer deposition of MoO_x for silicon heterojunction solar cells, Phys. Status Solidi RRL 9 (2015) 393–396.
[43] J. Melskens, *et al.*, (In preparation), 2018.
[44] S.E. Potts, W. Keuning, E. Langreis, G. Dingemans, M.C.M. van de Sanden, W.M.M. Kessels, Low temperature plasma-enhanced atomic layer deposition of metal oxide thin films, J. Electrochem. Soc. 157 (7) (2010) P66–P74.
[45] M.F.J. Vos, B. Macco, N.F.W. Thissen, A.A. Bol, W.M.M. Kessels, Atomic layer deposition of molybdenum oxide from $(N^tBu)_2(NMe_2)_2Mo$ and O_2 plasma, J. Vac. Sci. Technol. A 34 (1) (2016) (p. 01A103-1–01A103-7).
[46] Y. Wu, P.M. Hermkens, B.W.H. van de Loo, H.C.M. Knoops, S.E. Potts, M.A. Verheijen, F. Roozeboom, W.M.M. Kessels, Electrical transport and Al doping efficiency in nano scale ZnO films prepared by atomic layer deposition, J. Appl. Phys. 114 (2) (2013) 24308.
[47] D. Garcia-Alonso, S.E. Potts, C.A.A. van Helvoirt, M.A. Verheijen, W.M.M. Kessels, Atomic layer deposition of B-doped ZnO using triisopropyl borate as the boron precursor and comparison with Al-doped ZnO, J. Mater. Chem. C 3 (13) (2015) 3095–3107.
[48] B. Macco, H.C.M. Knoops, M.A. Verheijen, W. Beyer, M. Creatore, W.M.M. Kessels, Atomic layer deposition of high-mobility hydrogen-doped zinc oxide, Sol. Energy Mater. Sol. Cells 173 (2017) 111–119.
[49] W. Kern, Cleaning solutions based on hydrogen peroxide for use in silicon semiconductor technology, RCA Rev. 31 (. 1970) 187–206.
[50] S. Mack, A. Wolf, C. Brosinsky, S. Schmeisser, A. Kimmerle, P. Saint-Cast, M. Hofmann, D. Biro, Silicon surface passivation by thin thermal oxide/PECVD layer stack systems, IEEE J. Photovolt. 1 (2011) 135–145.
[51] A.G. Aberle, Advanced Surface Passivation and Analysis, Center for Photovoltaic Engineering, University of New South Wales, Sydney, NSW, Australia, 1999.
[52] C. Battaglia, S. Martín de Nicolas, S. de Wolf, X. Yin, M. Zheng, C. Ballif, A. Javey, Silicon heterojunction solar cell with passivated hole selective MoO_x contact, Appl. Phys. Lett. 104 (113902) (2014).
[53] J. Geissbühler, et al., 22.5% efficient silicon heterojunction solar cell with molybdenum oxide hole collector, Appl. Phys. Lett. 107 (081601) (2015).
[54] L.G. Gerling, S. Mahato, A. Morales-Vilches, G. Masmitja, P. Ortega, C. Voz, R. Alcubilla, J. Puigdollers, Transition metal oxides as hole-selective contacts in silicon heterojunction solar cells, Sol. Energy Mater. Sol. Cells 145 (part 2) (2016) 109–115.
[55] L.G. Gerling, C. Voz, R. Alcubilla, J. Puigdollers, Origin of passivation in hole-selective transition metal oxides for crystalline silicon heterojunction solar cells, J. Mater. Res 22 (2) (2016) 260–268.
[56] J. Bullock, A. Cuevas, T.G. Allen, C. Battaglia, Molybdenum oxide MoO_x: a versatile hole contact for silicon solar cells, Appl. Phys. Lett. 105 (232109) (2014).
[57] C. Battaglia, X. Yin, M. Zheng, I.D. Sharp, T. Chen, S. McDonnell, A. Azcatl, C. Carraro, B. Ma, R. Maboudian, R.M. Wallace, A. Javey, Hole selective MoO_x contact for silicon solar cells, Nano Lett. 14 (2014) 967–971.
[58] A. Laades, H.-P. Sperlich, M. Bähr, U. Stürzebecher, C.A. Diaz Alvarez, M. Burkhardt, H. Angermann, M. Blech, A. Lawerenz, On the impact of interfacial SiO_x-layer on the passivation properties of PECVD synthesized aluminum oxide, Phys. Status Solidi C 9 (10–11) (2012) 2120–2123.
[59] R.R. Razouk, B.E. Deal, Dependence of interface state density on silicon thermal oxidation process variables, J. Electrochem. Soc. 126 (9) (1979) 1573–1581.
[60] A. Moldovan, F. Feldmann, G. Krugel, M. Zimmer, J. Rentsch, M. Hermle, A. Roth-Fölsch, K. Kaufmann, C. Hagendorf, Simple cleaning and conditioning of silicon surfaces with UV/ozone sources, Energy Procedia 55 (2014) 834–844.
[61] H. Angermann, Conditioning of Si-interfaces by wet-chemical oxidation: electronic interface properties study by surface photovoltage measurements, Appl. Surf. Sci. 312 (2014) 3–16.
[62] N. Grant, K. Mcintosh, A review on low temperature chemically formed silicon dioxide for solar cell applications, in: Proceedings of 48th AuSES Annual Conference, 2010, pp. 1–10.
[63] G. Dingemans, C.A.A. van Helvoirt, D. Pierreux, W. Keuning, W.M.M. Kessels, Plasma-assisted ALD for the conformal deposition of SiO_2: process, material and electronic properties, J. Electrochem. Soc. 159 (2012) H277–H285.
[64] T. Asuha, O. Kobayashi, M. Maida, M. Inoue, Y. Takahashi, Todokoro, H. Kobayashi, Ultrathin silicon dioxide layers with a low leakage current density formed by chemical oxidation of Si, Appl. Phys. Lett. 81 (18) (2002) 3410–3412.
[65] T. Asuha, M. Kobayashi, H. Takahashi, Iwasa, H. Kobayashi, Spectroscopic and electrical properties of ultrathin SiO_2 layers formed with nitric acid, Surf. Sci. 547 (2003) 275–283.
[66] M. Morita, T. Ohmi, E. Hasegawa, A. Teramoto, Native oxide growth on silicon surface in ultrapure water and hydrogen peroxide, Jpn. J. Appl. Phys. 29 (12) (1990) L2392–L2394.
[67] A. Moldovan, F. Feldmann, M. Zimmer, J. Rentsch, J. Benick, M. Hermle, Tunnel oxide passivated carrier-selective contacts based on ultra-thin SiO_2 layers, Sol. Energy Mater. Sol. Cells 142 (2015) 123–127.
[68] V.D. Mihailetchi, Y. Komatsu, L.J. Geerligs, Nitric acid pretreatment for the passivation of boron emitters for n-type base silicon solar cells, Appl. Phys. Lett. 92 (063510) (2008).

[69] F. Feldmann, M. Bivour, C. Reichel, M. Hermle, S.W. Glunz, Passivated rear contacts for high-efficiency n-type Si solar cells providing high interface passivation quality and excellent transport characteristics, Sol. Energy Mater. Sol. Cells 120 (2014) 270–274.
[70] A. Richter, et al., n-Type Si solar cells with passivating electron contact: identifying sources for efficiency limitations by wafer thickness and resistivity variation, Sol. Energy Mater. Sol. Cells 173 (2017) 96–105.
[71] M. Rienäcker, et al., Recombination behavior of photolithography-free back junction back contact solar cells with carrier-selective polysilicon on oxide junctions for both polarities, Energy Procedia 92 (2016) 412–1361.
[72] G. Yang, A. Ingenito, N. van Hameren, O. Isabella, M. Zeman, Design and application of ion-implanted polySi passivating contacts for interdigitated back contact c-Si solar cells, Appl. Phys. Lett. 108 (033903) (2016).
[73] S. Bordihn, P. Engelhart, V. Mertens, G. Kesser, D. Köhn, G. Dingemans, M.M. Mandoc, J.W. Müller, W.M.M. Kessels, High surface passivation quality and thermal stability of ALD Al_2O_3 on wet chemical grown ultra-thin SiO_2 on silicon, Energy Procedia 8 (2011) 654–659.
[74] G. Dingemans, R. Seguin, P. Engelhart, M.C.M. van de Sanden, W.M.M. Kessels, Silicon surface passivation by ultrathin Al_2O_3 films synthesized by thermal and plasma atomic layer deposition, Phys. Status Solidi 4 (2010) 10–12.
[75] F. Werner, B. Veith, D. Zielke, L. Kühnemund, C. Tegenkamp, M. Seibt, R. Brendel, J. Schmidt, Electronic and chemical properties of the c-Si/Al_2O_3 interface, J. Appl. Phys. 109 (113701) (2011).
[76] P. Saint-Cast, Y.-H. Heo, E. Billot, P. Olwal, M. Hofmann, J. Rentsch, S.W. Glunz, R. Preu, Variation of the layer thickness to study the electrical property of PECVD Al_2O_3 / c-Si interface, Energy Procedia 8 (2011) 642–647.
[77] N.M. Terlinden, G. Dingemans, M.C.M. van de Sanden, W.M.M. Kessels, Role of field-effect on c-Si surface passivation by ultrathin (2–20 nm) atomic layer deposited Al_2O_3, Appl. Phys. Lett. 96 (112101) (2010).
[78] S. de Wolf, A. Descoeudres, Z.C. Holman, C. Ballif, High-efficiency silicon heterojunction solar cells: a review, Green 2 (2012) 7–24.
[79] G. Dingemans, F. Einsele, W. Beyer, M.C.M. van de Sanden, W.M.M. Kessels, Influence of annealing and Al_2O_3 properties on the hydrogen-induced passivation of the Si/SiO_2 interface, J. Appl. Phys. 111 (093713) (2012).
[80] B. Nemeth, D.L. Young, M.R. Page, V. LaSalvia, S. Johnston, R. Reedy, P. Stradins, Polycrystalline silicon passivated tunneling contacts for high efficiency silicon solar cells, J. Mater. Res. 31 (6) (. 2016) 671–681.
[81] G. Dingemans, W. Beyer, M.C.M. van de Sanden, W.M.M. Kessels, Hydrogen induced passivation of Si interfaces by Al_2O_3 films and SiO_2/Al_2O_3, Appl. Phys. Lett. 97 (152106) (2010).
[82] M.K. Stodolny, et al., N-type polysilicon passivating contact for industrial bifacial n-type solar cells, Sol. Energy Mater. Sol. Cells 158 (2016) 24–28.
[83] A.F. Thomson, K.R. McIntosh, Light-enhanced surface passivation of TiO_2-coated silicon, Prog. Photovolt.: Res. Appl. 20 (2012) 342–349.
[84] B. Macco, J.H. Bivour, S.B. Basuvalingam, L.E. Black, J. Melskens, W.M.M. Kessels (Erwin), Effective passivation of silicon surfaces by ultrathin atomic-layer deposited niobium oxide, Appl. Phys. Lett. 112 (24) (2018) 242105, https://doi.org/10.1063/1.5029346.
[85] L.E. Black, W.M.M. Kessels, Investigation of crystalline silicon surface passivation by positively charged PO_x/Al_2O_3 stacks, Sol. Energy Mater. Sol. Cells 185 (2018) 385–391, https://doi.org/10.1016/j.solmat.2018.05.007.